PROCEEDINGS OF SCIENCE

# Contribution of young massive stellar clusters to the Galactic diffuse neutrino and $\gamma$-ray emissions

**S. Menchiari,**[a,b] **S. Celli,**[c,d] **R. Lopez-Coto,**[a] **G. Morlino,**[b] **G. Peron**[b] **and V. Vecchiotti**[b,e]

[a] *Instituto de Astrofísica de Andalucía, Glorieta de la Astronomía s/n, 18008, Granada, Spain*
[b] *Istituto Nazionale di Astrofisica, Osservatorio Astrofisico di Arcetri, L.go E. Fermi 5, Firenze, Italy*
[c] *Sapienza Università di Roma, Physics Department, P.le Aldo Moro 5, 00185, Rome, Italy*
[d] *Istituto Nazionale di Fisica Nucleare, Sezione di Roma, P.le Aldo Moro 5, 00185, Rome, Italy*
[e] *NTNU, Department of Physics, NO-7491 Trondheim, Norway*

*E-mail:* smenchiari@iaa.es

Young massive stellar clusters (YMSCs) have emerged as energetic non-thermal sources, after the recent observation of extended $\gamma$-ray emission by a dozen YMSCs. The large size of their gamma-ray halos, of the order of the excavated bubble from the collective wind, makes the detection of individual YMSCs rather challenging because of the low surface brightness. As a result, the emission from most of the Galactic YMSCs could be unresolved, thus contributing to the diffuse $\gamma$-ray radiation and neutrino flux observed along the Galactic Plane. In this study, we estimate that possible contribution of the population of YMSCs to the Galactic diffuse radiative emissions, by simulating synthetic samples of these sources resembling the observed properties of local clusters. We compute the resulting secondary emission from hadronic interactions occurring in each cluster by particles accelerated at the cluster's collective wind termination shock and at the supernovae exploded in the core, and compare them with available diffuse $\gamma$-ray and neutrino observations by different experiments, including ARGO, LHAASO, and IceCube.

39th International Cosmic Ray Conference (ICRC2025)
15–24 July 2025
Geneva, Switzerland

© Copyright owned by the author(s) under the terms of the Creative Commons Attribution-NonCommercial-NoDerivatives 4.0 International License (CC BY-NC-ND 4.0).



PoS(ICRC2025)1010

## 1. Introduction

Young massive star clusters (YMSCs) are nowadays recognized as a new class of cosmic-ray (CRs) factories. The powerful winds from Wolf-Rayet and OB-type stars, as well as supernova (SN) explosions occurring in the cluster core provide the ideal environment for particle acceleration [13]. The presence of freshly injected CRs has been demonstrated by the detection of non-thermal high energy radiation observed in coincidence with several objects [2, 4, 26]. In some cases, the radiation is explained by considering a hadronic emission process [3, 26]. One of the peculiarity about the $\gamma$-ray emission from YMSCs, is that the emission appears to be extended, with a size that well correlates with the projected dimension of the wind-blown bubble generated by the feedback of the stellar winds. This fact suggests that the emission from YMSCs is characterized by a low surface brightness, which can induce a bias in the detection of high energy radiation from this class of sources. If this is the case, then, the emission from most of the galactic YMSCs is not resolved, and end up to contribute to diffuse $\gamma$-ray emission observed along the galactic plane. Recently, a combined analysis of Fermi-LAT and LHAASO data has shown that an extra component related to one or possible multiple populations of unresolved sources, is necessary to reproduce the observed $\gamma$-ray spectrum [30]. However, specific models for particle propagations [11], as well as a correct estimation of the CR sea emission that accounts for the uncertainties on the gas distribution and cross section [29], are still able to reproduce the observed galactic diffuse emission. Estimating the contribution of non-resolved sources becomes then crucial for modelling the Galactic diffuse emission and to correctly understand the physics of particle propagation in the Milky Way. In a recent work, [21] has demonstrated that YMSCs are likely important contributors to such emission and that they can potentially explain, in large part, the extra component invoked to reproduce the observed spectra.

In this work, we propose to extend the study of [21] by evaluating the contribution of YMSCs to the Galactic neutrino emission, with the goal of determining whether the expected signal is consistent with the observed flux. This will also provide a better estimate to the contribution YMSCs to the galactic diffuse $\gamma$-ray emission. To do so, we follow the same approach of [21], which involves generating synthetic populations of YMSCs based on the properties of observed local clusters. For each synthetic cluster, a mock stellar population is simulated in order to determine the parameters of the collective cluster wind. Afterward, the CR content in each cluster is calculated using the model of particle acceleration at the cluster wind termination shock [23]. We also consider various scenarios for the plasma turbulence inside the wind-blown bubbles in order to model different possible CR spectra. We then estimate the resulting neutrino and $\gamma$-ray emission from hadronic interactions and compare it with current measurements from IceCube [15], ARGO [5], and LHAASO [8, 9]. Several improvements has been added to the method, such as the inclusion of the contribution of particle acceleration by SNe occurring in the cluster (as well as their power injected in the calculation of the properties of the wind blown bubbles), and a more realistic model for the target gas density distribution.



PoS(ICRC2025)1010

## 2. Simulation of the synthetic star cluster population

The population of YMSCs is only known locally, within $\lesssim$ 2 kpc from the Solar System. In order to estimate the contribution of all the galactic YMSCs neutrino and $\gamma$-ray emission, it is necessary to first calculate the number of YMSCs and then simulate the population. Both the calculations for the estimations of the number of YMSCs and the process for the simulations are detailed in [21], we here provide a brief summary of the entire methodology as well as a description of few newly introduced improvements.

We consider star clusters with masses ranging between $1 - 64$ kM$_\odot$, and ages below 30 Myr. The choice of the minimum mass is justified by the fact that YMSCs with lower mass possess very low wind power, i.e do not produce a significant amount of CRs, while the upper mass bound is constrained by the maximum cluster mass observed in the Milky Way [27]. The maximum age is instead chosen as it is the time at which a 8 M$_\odot$ is expected to explode as a SN [7], consequently, clusters older than 30 Myr do not host a relevant number of core collapse SN and the CR production is significantly suppressed. The number of YMSCs within the chosen mass and age intervals are calculated by integrating the cluster formation rate, defined as: $\xi_{\rm sc}(M_{\rm sc}, t, r) = \psi(t)\, f(M_{\rm sc})\, \rho(r)$, where $\psi(t)$, $f(M_{\rm sc})$ and $\rho(r)$ are, in order, the local cluster formation rate, the cluster initial mass function and the cluster spatial distribution. The local cluster formation rate (constant in the last 30 Myrs) is estimated from the star formation rate in measured in embedded clusters [6], while $f(M_{\rm sc})$ is calculated using the census of the Global Star Clusters Survey [27]. Regarding the cluster spatial distribution, we here assume that is traced by the Galactocentric position of giant molecular clouds, which we estimate using the catalogue provided by [14]. The integration of $\xi_{\rm sc}(M_{\rm sc}, t, r)$ returns a total 2243 YMSCs. For each of these object, we randomly extract mass, age and galactocentric distance using the probability distributions $f(M_{\rm sc})$, $\psi(t)$, and $\rho(r)$ respectively. Then, knowing the galactocentric distance, each cluster is displaced so as to reproduce the observed spiral structure of the Milky Way [14]. The method is described in [21].

After assigning a mass and age to each YMSC, we generate a mock stellar population by randomly sampling the initial mass function [18]. We then exclude stars that have already exploded as SNe from a stellar cluster by removing all stars with a turn-off time (age at which a star of a certain mass leave the main sequence [7]) shorter than the cluster's age. Post-main-sequence evolution is neglected, except in the case of Wolf-Rayet stars. Specifically, we assume that all stars with $M_\star > 25$ M$\odot$ enter a Wolf-Rayet phase lasting approximately 0.3 Myr following their turn-off time. For each main sequence stars left in the population, we calculate its corresponding wind power and mass loss rate using a pure empirical approach [19, 24]. In a similar way, also the power and mass loss rate of Wolf-Rayet stars is calculated [25]. Finally, the wind power, mass loss rate and wind speed of the collective cluster wind are $L_w = \sum_i L_{\star,i}$, $\dot{M} = \sum_i \dot{M}_{\star,i}$, and $v_w = \sqrt{2L_w/\dot{M}}$; where $L_{\star,i}$ and $\dot{M}_{\star,i}$ are the wind power an mass loss rate of every mock star. With these parameter it is possible to obtain the structure of the wind blown bubble, i.e. the radius of the termination shock ($R_{ts}$), the radius of the forward shock ($R_{fs}$) and the radius of the contact discontinuity separating the dense swept-up shell from the hot shocked wind material ($R_{cd} = 0.9R_{fs}$). When calculating these values, we use a modified version of the classical Weaver model that accounts for the energy losses by radiation and conduction cooling. This is done by reducing the available power of the system by a factor $\eta_m = 0.1$ [see Sec 2 in 22]. Differently from the method used in [21], we also



PoS(ICRC2025)1010

include in the power of the system the additional luminosity injected by the SNe. Assuming that each SN release a total energy of $E_{SN} = 10^{51}$ erg, so that the total power of the cluster becomes $L_{tot} = L_w + N_{SN}E_{SN}/t$, where $N_{SN}$ and $t$ are the number of SN exploded in the cluster and the age of the cluster.

## 3. Cosmic-ray production in YMSCs

We model the CR production assuming that particles are accelerated at the collective cluster wind termination shock [23]. The CR distribution in the system is obtained after solving the steady state transport equation in radial symmetry. The solution is totally analythical and its expression reads:

$$f_{cr}(r,p) = (f_{ts}(p,D) + < f_{SN}(p) >)\,\Gamma(r,p,D) \tag{1}$$

where $f_{ts}(p)$ is the spectrum of particles accelerated at the cluster wind termination shock [see Sec. 3.2 in 20], $< f_{SN}(p) >$ is the spectrum of CR injected by SN explosions [see Sec. 3.2 in 22], and $\Gamma(r,p,D)$ is a function that accounts how particles propagates in the different zone of the bubble [see Sec. 3.2 in 20]. Both $f_{ts}$ and the function $\Gamma$ depends on the diffusion coefficient $D$ in the system. We here consider three distinct scenarios reflecting three possible recipes for the diffusion coefficient, that are related to the type of plasma turbulence spectrum in the bubble: Kolmogorov, Kraichnan and Bohm. Note that when calculating $\langle f_{\rm SN}(p)\rangle$, we only include SNe that have exploded within an advection time, defined as $t_{\rm adv} = \int_{R_b}^{R_{\rm ts}} \frac{dr}{u(r)}$, ensuring that the particles they inject are still confined within the bubble. The contribution from older SNe should not be taken into account, as the cosmic rays they accelerated are expected to have already escaped the system. The inclusion of the term $< f_{SN}(p) >$ is a further improvement of the method presented in [21].

## 4. Diffuse neutrino and $\gamma$-ray emission

The neutrino ($\phi_\nu$) and $\gamma$-ray ($\phi_\gamma$) flux from each YMSC is calculated as:

$$\phi_{\nu,\gamma}(E_{\nu,\gamma}) = \frac{c}{d^2}\int\int_0^{R_{\rm b}} r^2 f_{cr}(r,E_p) n(r) \frac{d\sigma_{\nu,\gamma}(E_p,E_{\nu,\gamma})}{dE_p} dr dE_p\,, \tag{2}$$

where $d$ is the distance from the Solar System, $c$ is the speed of light, $E_p$ is the kinetic energy of CRs, and $d\sigma_{\nu,\gamma}/dE_p$ is the differential cross section for $\gamma$-ray [16] production, or the all-flavour neutrino production [17]. The function $n(r)$ represents the distribution of target density in the wind blown bubble.

$$n(r) = \left[\frac{\dot{M}}{4\pi R_{ts}^2 v_w m_p} \quad \text{for } r \le R_{ts}; \quad \frac{\dot{M}_{sh}+\dot{M}}{V_b m_p} t \quad \text{for } R_{ts} < r \le R_{cd}; \quad \frac{M_s}{V_s m_p} \text{for } R_{cd} < r \le R_{fs}\right] \tag{3}$$

where $m_p$ is the proton mass, $\dot{M}_{sh}$ is the mass evaporation rate of the swept-up shell [10], $V_b = 4/3\pi(R_{cd}^3 - R_{ts}^3)$ is the volume of the shocked wind region, $V_s$ is the shell volume, and $M_s = 4/3\pi R_{fs}^3 \rho_0$ is the mass of swept up material, with $\rho_0$ as the mass density of the ambient medium in which the bubble expands. Finally, we model the spatial template of each YMSCs assuming that the flux calculated in Eq. 2 comes from a circular region with size equal to $R_{fs}$.



PoS(ICRC2025)1010

The total all-sky diffuse neutrino flux is calculated by simply adding to the propagating CR sea emission ($\phi_{\nu,sea}$) the flux sum over the entire population of YMSCs: $\phi_{\nu,tot} = \phi_{\nu,sea} + \sum_i \phi_{\nu,i}$, where $\phi_{\nu,i}$ is the flux of the $i$-th cluster. We consider several possible spectra for $\phi_{\nu,\mathrm{sea}}$, all based on the assumption of a spatially constant Galactic CR spectrum [29]. Specifically, we adopt two CR spectral models [12, 29], representing lower and upper bounds. The lower bound corresponds to a fit to the CR spectrum measured by the IceTop experiment [1], while the upper bound is based on the spectrum measured by KASCADE [28]. Finally, the all-flavour $\phi_{\nu,\mathrm{tot}}$ is rescaled by a factor of 3 to account for the flavour composition of the events detected by IceCube.

The diffuse $\gamma$-ray flux is obtained after removing the regions of the galactic plane where the emission from YMSCs is resolved. This is done by masking all the positions in the sky where the flux at 100 TeV from YMSCs is expected to be detected by LHAASO with a significance higher than $5\sigma$ [see Appendix B in 21]. We also systematically mask the inner part of the galactic plane ($l \leq 70°$ and $|b| < 1.5°$) so as to mimic the removal of other types of $\gamma$-ray sources (such as pulsar wind nebulae or supernova remnants) that are not simulated in this work. On top of the emission from unresolved YMSCs, we sum the Galactic diffuse flux (similarly masked), which is obtained using the same CR spectra employed in the calculation of the neutrino emission.

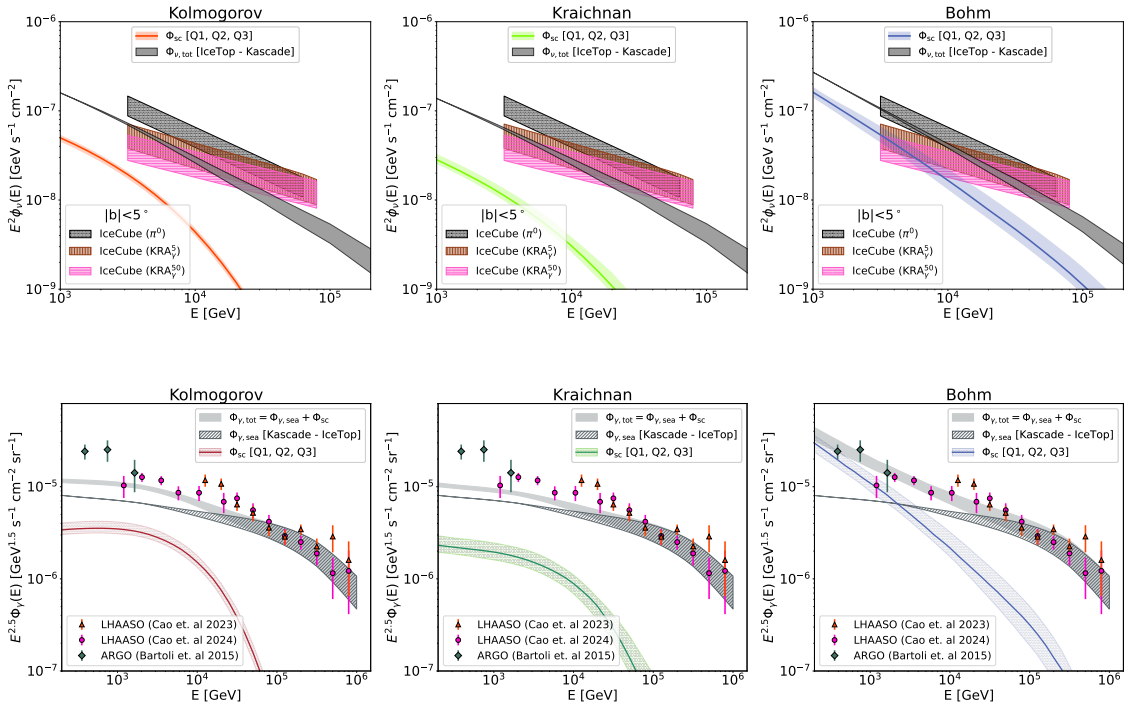


**Figure 1:** Top row: Total diffuse neutrino flux (shaded grey band). The solid coloured lines and the associated shaded regions show the predicted emission from YMSCs under the three different diffusion regimes considered: Kolmogorov (left), Kraichnan (center), and Bohm (right). The solid line represent the median (second quartile, Q2) flux obtained after simulating 100 different synthetic populations, while the width of the associated shaded band represents the first (Q1) and third (Q3) quartile. The hatched regions indicate the diffuse neutrino flux measured by IceCube within a region with latitude $|b| < 5°$. Bottom row: Total diffuse $\gamma$-ray flux (shaded grey area), including both the emission from YMSCs (solid line and dashed region) and the contribution from the Galactic CR sea (grey dashed band). The model predictions are compared with observations from ARGO [5] and LHAASO [8, 9].



PoS(ICRC2025)1010

## 5. Discussion and conclusions

The comparison between both the measured galactic neutrino flux and diffuse $\gamma$-ray emission with our estimates is shown in Fig. 1. It can be clearly see that the total expected emission is fully consistent with the observed data, from both the neutrino and $\gamma$-ray side. We can quantify the importance of the neutrino flux from YMSCs by comparing it to the CR sea diffuse emission, i.e, by calculating $\phi_{\nu,sc}/\phi_{\nu,sea}$, where $\phi_{\nu,sc} = \sum_i \phi_{\nu,i}$. The fraction is $\lesssim$ 15% at energies of $\sim$ 10 TeV for the Kolmogorov and Kraichnan scenarios, while the rise up to $\sim$ 60% when the Bohm diffusion is considered. A similar comparison can be made with the $\gamma$-ray flux, finding that the unresolved emission from YMSCs at 1 TeV is $\sim$ 50%, $\sim$ 30% and $\sim$ 150% that of the CR sea for the Kolmogorov, Kraichnan and Bohm scenarios respectively.

We conclude that unresolved YMSCs represent significant contributors to the Galactic diffuse $\gamma$-ray emission at energies of a few TeV, and that the neutrino flux ranges between 10% to 60% of the emission expected from the CR sea.

## References


[1] Aartsen M. G., et al., 2019, Phys. Rev. D, 100, 082002

[2] Abeysekara A. U., et al., 2021, Nature Astronomy, 5, 465

[3] Aharonian F., Yang R., de Oña Wilhelmi E., 2019, Nature Astronomy, 3, 561

[4] Aharonian F., et al., 2022, A&A, 666, A124

[5] Bartoli B., et al., 2015, ApJ, 806, 20

[6] Bonatto C., Bica E., 2011, MNRAS, 415, 2827

[7] Buzzoni A., 2002, AJ, 123, 1188

[8] Cao Z., et al., 2023, Phys. Rev. Lett., 131, 151001

[9] Cao Z., et al., 2025, Phys. Rev. Lett., 134, 081002

[10] Castor J., McCray R., Weaver R., 1975, ApJ, 200, L107

[11] De La Torre Luque P., Gaggero D., Grasso D., Marinelli A., Rocamora M., 2025, arXiv e-prints, p. arXiv:2502.18268

[12] Dembinski H., Engel R., Fedynitch A., Gaisser T. K., Riehn F., Stanev T., 2017, in 35th International Cosmic Ray Conference (ICRC2017). p. 533 (arXiv:1711.11432), doi:10.22323/1.301.0533

[13] Gabici S., 2024, in 7th Heidelberg International Symposium on High-Energy Gamma-Ray Astronomy. p. 16 (arXiv:2301.06505), doi:10.48550/arXiv.2301.06505

[14] Hou L. G., Han J. L., 2014, A&A, 569, A125

[15] Icecube Collaboration et al., 2023, Science, 380, 1338

[16] Kafexhiu E., Aharonian F., Taylor A. M., Vila G. S., 2014, Phys. Rev. D, 90, 123014

[17] Koldobskiy S., Kachelrieß M., Lskavyan A., Neronov A., Ostapchenko S., Semikoz D. V., 2021, Phys. Rev. D, 104, 123027

[18] Kroupa P., 2001, MNRAS, 322, 231

[19] Kudritzki R.-P., Puls J., 2000, ARA&A, 38, 613

[20] Menchiari S., Morlino G., Amato E., Bucciantini N., Beltrán M. T., 2024, A&A, 686, A242

[21] Menchiari S., Morlino G., Amato E., Bucciantini N., Peron G., Sacco G., 2025, A&A, 695, A175

[22] Mitchell A. M. W., Morlino G., Celli S., Menchiari S., Specovius A., 2024, arXiv e-prints, p. arXiv:2403.16650

[23] Morlino G., Blasi P., Peretti E., Cristofari P., 2021, MNRAS, 504, 6096

[24] Nieuwenhuijzen H., de Jager C., 1990, A&A, 231, 134

[25] Nugis T., Lamers H. J. G. L. M., 2000, A&A, 360, 227

[26] Peron G., Casanova S., Gabici S., Baghmanyan V., Aharonian F., 2024, Nature Astronomy

[27] Piskunov A. E., Just A., Kharchenko N. V., Berczik P., Scholz R. D., Reffert S., Yen S. X., 2018, A&A, 614, A22

[28] The KASCADE-Grande Collaboration et al., 2013, arXiv e-prints, p. arXiv:1306.6283

[29] Vecchiotti V., Peron G., Amato E., Menchiari S., Morlino G., Pagliaroli G., Villante F. L., 2024, arXiv e-prints, p. arXiv:2411.11439

[30] Zhang R., Huang X., Xu Z.-H., Zhao S., Yuan Q., 2023, ApJ, 957, 43


PoS(ICRC2025)1010